

# **Grazing incidence reflection coefficients of rhodium, osmium, platinum, and gold from 50 to 300 Å**

Michael C. Hettrick, Scott A. Flint, and Jerry Edelstein

Applied Optics Vol. 24, Issue 22, pp. 3682-3685 (1985)

<http://dx.doi.org/10.1364/AO.24.003682>

© 1985 Optical Society of America. One print or electronic copy may be made for personal use only. Systematic reproduction and distribution, duplication of any material in this paper for a fee or for commercial purposes, or modifications of the content of this paper are prohibited.

$$n_c = \left[ \epsilon_\infty + \frac{i\omega_p^2/(\omega_r\omega)}{1 - i\omega/\omega_r} \right]^{1/2}, \quad (6)$$

$$\epsilon_c = \epsilon_\infty + \frac{i\omega_p^2/(\omega_r\omega)}{1 - i\omega/\omega_r}, \quad (7)$$

$$z_c = \frac{1}{\left[ \epsilon_\infty + \frac{i\omega_p^2/(\omega_r\omega)}{1 - i\omega/\omega_r} \right]^{1/2}}, \quad (8)$$

$$\sigma_c(\text{sec}^{-1}) = \frac{c\omega_p^2}{2\omega_r(1 - i\omega/\omega_r)} = \frac{\sigma_0(\text{sec}^{-1})}{1 - i\omega/\omega_r}, \quad (9)$$

where  $\epsilon_\infty$  is the real part of the high frequency dielectric function,  $\omega_p$  is the plasma frequency,  $\omega_r$  is the scattering frequency, and  $\sigma_0 = 1/\rho_0$  is the dc conductivity in esu ( $\text{sec}^{-1}$ ). The high frequency or optical conductivity is defined as

$$\sigma_{\text{opt}}(\text{sec}^{-1}) = 1/\rho_{\text{opt}}(\text{sec}) = \frac{c\omega_p^2}{2\omega_r} = \frac{10^{-9}c^2}{\rho_{\text{opt}}(\Omega \text{ cm})}. \quad (10)$$

If the simple Drude model were correct,  $\sigma_{\text{opt}}$  should equal  $\sigma_0$ . However, for many metals this is not true.<sup>8,9</sup>

The real and imaginary parts of  $n_c$ ,  $\epsilon_c$ ,  $z_c$ , and  $\sigma_c$  are given in Table II for the Drude model. Also shown in Table II are the expressions for  $\omega_r$  and  $\omega_p$  and  $\rho_{\text{opt}}$ , the real part of the complex resistivity.

The plasma frequency  $\omega_p$  and scattering frequency  $\omega_r$  are related to the electron density  $N$  ( $\text{cm}^{-3}$ ) and the electron scattering time  $\tau$  (sec) by

$$\omega(\text{cm}^{-1}) = \omega(\text{rad/sec})/(2\pi c), \quad (11)$$

$$\omega_r(\text{cm}^{-1}) = 1/[2\pi c\tau(\text{sec})], \quad (12)$$

and<sup>3</sup>

$$\omega_p(\text{cm}^{-1}) = [Ne^2/(\pi c^2 m^*)]^{1/2}, \quad (13)$$

where  $m^*$  (g) is the effective mass of the electrons, and  $e$  is the electron charge in esu.

Table III gives the reflectance at a vacuum-medium interface for normal incidence. Also shown is the same reflectance for a Drude model material. For this equation (and only this equation), the approximation

$$\epsilon_\infty \ll [(\omega_p^2/\omega_r^2)/(1 + \omega^2/\omega_r^2)] \quad (14)$$

has been made. In general, for a metal, this approximation holds to better than 1% for frequencies of  $<10^3 \text{ cm}^{-1}$ .

The information in these tables can be used to obtain other frequently used quantities in terms of  $n_c$ ,  $\epsilon_c$ ,  $z_c$ , or  $\sigma_c$ . For example, the absorption coefficient  $\alpha$  given by

$$\alpha = 4\pi k\omega \quad (15)$$

can be obtained in terms of the components of  $\epsilon_c$ ,  $z_c$ , or  $\sigma_c$  using line 4 of Table I. The relations<sup>8,9</sup>

$$\omega_r = \frac{\omega\epsilon_2}{\epsilon_\infty - \epsilon_1}, \quad (16)$$

$$\omega_p^2 = (\epsilon_\infty - \epsilon_1)(\omega_r^2 + \omega^2) = \omega^2 \left[ \frac{(\epsilon_\infty - \epsilon_1)^2 + \epsilon_2^2}{\epsilon_\infty - \epsilon_1} \right] \quad (17)$$

can be obtained from lines 9 and 10 of Table II. Equations (16) and (17) are a way to find the Drude model parameters  $\omega_r$  and  $\omega_p$  at a given frequency.

This work was partially supported by the U.S. Army [DAAA-15-85-K-0004 (M. Milham)]. We wish to thank Lola Cook for typing the tables.

## References

1. F. Wooten, *Optical Properties of Solids* (Academic, New York, 1972), p. 90ff.
2. J. D. Jackson, *Classical Electrodynamics* (Wiley, New York, 1975), p. 296.
3. C. Kittel, *Introduction to Solid State Physics* (Wiley, New York, 1976), Chap. 10.
4. A. H. Wilson, *The Theory of Metals* (Cambridge U. P. London, 1953).
5. B. Donovan, *Elementary Theory of Metals, Vol. 2*, in *The International Encyclopedia of Physical Chemistry and Chemical Physics*, Topic 11; *The Ideal Crystalline State*, M. Blackman, Ed. (Pergamon, Oxford, 1967). Note, he uses waves of the form  $\exp[i(-\mathbf{q} \cdot \mathbf{r} + 2\pi c\omega t)]$ .
6. F. E. Pinkerton and A. J. Sievers, "Quantitative FIR Absorptivity Measurements of Metals with Dual Non-Resonant Cavities," *Infrared Phys.* **22**, 377 (1982).
7. J. Stone, *Radiation and Optics* (McGraw-Hill, New York, 1963).
8. M. A. Ordal, L. L. Long, R. J. Bell, S. E. Bell, R. R. Bell, R. W. Alexander, Jr., and C. A. Ward, "Optical Properties of the Metals Al, Co, Cu, Au, Fe, Pb, Ni, Pd, Pt, Ag, Ti, and W in the Infrared and Far Infrared," *Appl. Opt.* **22**, 1099 (1983).
9. M. A. Ordal, R. J. Bell, R. W. Alexander, Jr., and M. R. Querry, "Optical Properties of Fourteen Metals in the Infrared and Far Infrared: Al, Co, Cu, Au, Fe, Pb, Mo, Ni, Pd, Pt, Ag, Ti, V, and W," *Appl. Opt.* **24**, (15 Dec. 1985).
10. S. Perkowitz, G. L. Carr, B. Subramaniam, and B. Mitrović, "Far-infrared Determination of Scattering Behavior and Plasma Frequency in  $\text{V}_3\text{Si}$ ,  $\text{Nb}_3\text{Ge}$ , and Nb," *Phys. Rev. B* **32**, 153 (1985).

## Grazing incidence reflection coefficients of rhodium, osmium, platinum, and gold from 50 to 300 Å

Michael C. Hettrick, Scott A. Flint, and Jerry Edelstein

Michael Hettrick is with University of California, Lawrence Berkeley Laboratory, Center for X-ray Optics, Berkeley, California 94720; S. A. Flint is with Acton Research Corporation, P.O. Box 215, Acton, Massachusetts 01720; and J. Edelstein is with University of California, Astronomy Department, Berkeley, California 94720.

Received 11 July 1985.

0003-6935/85/223682-04\$02.00/0.

© 1985 Optical Society of America.

In the design of soft x-ray and extreme UV instrumentation, it is often necessary to predict accurately the reflective throughput of optics. Longward of 300 Å, a large body of reflection data exists from which optical constants have been derived for most elements in the periodic table.<sup>1</sup> A similar compilation is available in the soft x ray (6–124 Å), based on atomic photoabsorption cross sections which dominate any optical response at these wavelengths.<sup>2</sup> However, due to the requirement of grazing incidence techniques below 300 Å combined with the fact that intense light sources are not widely available at these wavelengths, direct reflection measurements are sparse<sup>3–9</sup> in the interesting region from 50 to 300 Å. This data gap is apparent in a recent compilation of the optical constants for several metals from the X ray to the microwave.<sup>10</sup> The published data in this band are insufficient to provide optical designers with a comparison of coatings from which to choose a desired response.

We have carried out reflectance measurements of rhodium, osmium, platinum, and gold at multiple grazing angles of illumination and at 14 wavelengths between 46.5 and 283 Å.

All reflective coatings were deposited by e-beam evaporation onto a glass substrate which was at room temperature. The distance from the source (e-gun) to the substrate was 45.7 cm (18 in.), and the system resided in a 66-cm (26-in.) diam. stainless steel vacuum evaporator. Pressures during evaporation were typically  $1\text{--}5 \times 10^{-6}$  Torr. Film deposition rates ranged from  $\sim 5$  Å/sec for Os, Rh, and Pt to  $\sim 15$  Å/sec for Au. Each overcoating was 125 Å thick over a binding layer of 50 Å chromium. These thin coatings result in smooth surfaces, and yet, due to the use of glancing illumination, they are relatively opaque and thus immune from interference effects at the coating-substrate interface.<sup>11</sup> However, at the shortest wavelengths (50–100 Å) the critical angle of the coatings is smaller than the largest graze angle ( $16^\circ$ ) where we calculate<sup>2</sup> a transmission as large as 25%. This may result in somewhat lower reflectances than expected from opaque coatings.

The measurements were performed at Acton Research Corp. (ARC). The measurement system consisted of a Penning-type light source,<sup>12</sup> an ARC (1.5-m) grazing incidence monochromator, and an ARC reflectometer with a gas flow proportional counter. The light source provided emission lines due to sputtering from two aluminum cathodes placed at high voltage in an argon gas. In the 200–300 Å region, emission lines were also obtained from the discharges of a neon gas flowing between the cathodes. The monochromator was a Rowland circle concave grating with the light source placed on a scanning entrance slit and the reflectometer placed on an exit slit fixed at an  $86^\circ$  angle from the grating normal. The grating groove density ( $1200 \text{ mm}^{-1}$ ) and reflective coating (gold) allowed wavelength selection from zero order to 450 Å. An aperture slit preceded the sample to ensure underillumination at the most grazing angle of  $2^\circ$ . The reflectometer was capable of measuring reflectance at incidence angles from  $8^\circ$  to  $88^\circ$  ( $\pm 0.2^\circ$ ) and used a unique design which allowed the detector to be external to the vacuum system.

The gas proportional counter had a polypropylene window which permitted transmission from the carbon edge (45 Å) to  $\sim 200$  Å. For the longest wavelength measurements (200–300 Å), a Lexan window was used, and an aluminum/silicon thin-film filter was also inserted prior to the detector to eliminate second-order contamination.

The reflectance measurements were made in a point-by-point manner: (1) setting the monochromator to the desired wavelength; (2) measuring the straightthrough (direct) intensity with the sample removed from the beam; (3) inserting the sample; (4) rotating the sample and the detector to the desired angle; and (5) measuring the reflected intensity. The reflection coefficient was taken as the ratio of the reflected and direct counts over 40-sec integrations each. As the light source varied in intensity between measurements, the direct intensity was also measured after the reflection measurement to provide a base-line average intensity.

The detector background was measured by closing the entrance to the reflectometer between measurements and was consistently negligible compared to the intensity of the reflected beam. The off-line intensity of the light source dominated the background but was measured only intermittently due to practical constraints on time. For those measurements, the reflection coefficient of this background was verified to be close to that at the desired wavelength. However, due to significant time variability of the light source and possibly the line-to-background ratio, our inability to routinely subtract this background introduces the most uncertainty in our measurements. As all count rates were

$<5000$  counts/sec, corrections due to dead time of the detector electronics were not necessary.

As we were not equipped to measure polarization, its potential effect on the reflectance measurements was considered. Due to prior reflection by the monochromator grating, the light incident to the reflectance sample was linearly polarized to some degree along the grating grooves (S-polarization). As the grating and sample were situated to reflect within the same plane, this induced polarization will increase the reflectance of the sample. Using previously published optical constants<sup>4,5</sup> we find that a 100% linearly polarized beam onto the sample would enhance the reflectance by at most 5% absolute compared to unpolarized incident light. Since the grating is illuminated at a graze angle of  $6^\circ$ , which should result in only at most a 10% induced polarization, the effect on our measured sample reflectances should be small ( $<1\%$ ).

In Figs. 1–4, we present the reflection coefficients derived from this work. A quick glance at these plots reveals the expected general trend toward lower reflectances as the graze angle is increased or the wavelength shortened. However, an interesting deviation from this trend appears in all four coatings, being a reflectance peak extending from 100 to 160 Å and being most pronounced at large graze angles. The fact that the wavelength position of the peak does not shift as a function of graze angle disqualifies interference at the substrate boundary as the source of these bumps. Rather, they coincide with the absorption feature identified by Henke *et al.*,<sup>2</sup> as the  $5p\text{--}ed$  transition in each of the four elements. A peak in the absorption coefficient of gold at 140 Å has also been measured by Predehl *et al.*,<sup>13</sup> from transmission grating efficiencies. Such narrowband increase in reflectivity can be enhanced in multiple-bounce optical systems and be used to spectrally filter the incident light. A second notable point is that within the bump between 100 and 160 Å the reflectance is fairly insensitive to the value of graze angles  $<4^\circ$ . At these wavelengths, the measurement accuracy of 5–10% resulted in some anomalous data points in the comparative reflectance at 4 and  $2^\circ$ , as shown in Figs. 1, 3, and 4.

Averages of the measured reflectance values over the entire region from 47 to 283 Å revealed that rhodium has the highest overall reflectance of the four coatings measured following by osmium, gold, and platinum. The difference becomes more pronounced as the graze angle increases. For example, at  $16^\circ$ , rhodium outreflects gold by a factor of 1.3 on average. Gold and platinum are the most common overcoatings for gratings and mirrors used in the vacuum UV. Yet, from our measurements, significantly higher efficiencies are projected in the 50–300 Å region if the optics are overcoated with rhodium or osmium. These trends are consistent with published data at longer wavelengths,<sup>1,3,4</sup> where the reflectances reported here compare well within the region of overlap ( $\sim 150\text{--}280$  Å). However, at the shorter wavelengths, our reflectances are lower than expected. An independent set of measurements<sup>14</sup> on a rhodium flat at 114 Å showed  $\sim 15\%$  higher absolute reflectances than an average of our values at 104 and 124 Å. These higher reflectances are in agreement with those predicted by Henke *et al.*,<sup>2</sup> assuming a surface microroughness of 20 Å. The independent measurements were also made at 170 Å and resulted in reflectances of  $\sim 5\text{--}10\%$  higher absolute than those reported here.

The reflectance measurements of rhodium and osmium were repeated after several months had elapsed following the initial measurements plotted in Figs. 1 and 2. After six months, rhodium was remeasured at 2 and  $4^\circ$  graze angles and for wavelengths between 47 and 90.8 Å. It showed a

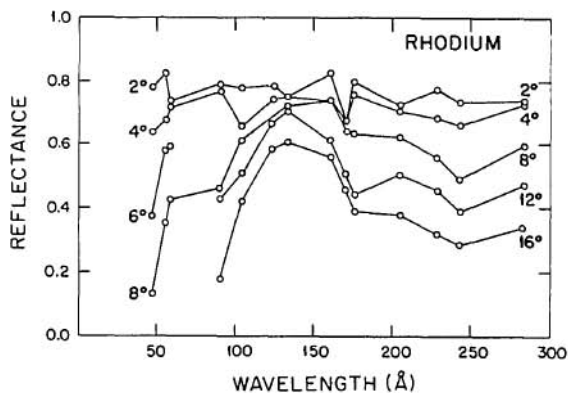


Fig. 1 Measured reflectance of rhodium as a function of wavelength (46–283 Å) and graze angle (2–16°). The measurement error is estimated to be  $\pm 10\%$  relative.

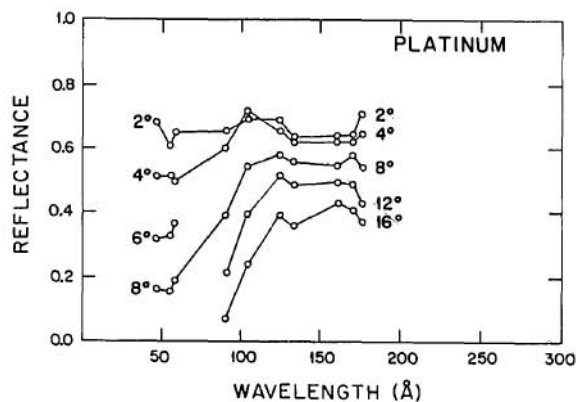


Fig. 3 Measured reflectance of platinum as a function of wavelength (46–283 Å) and graze angle (2–16°). The measurement error is estimated to be  $\pm 10\%$  relative.

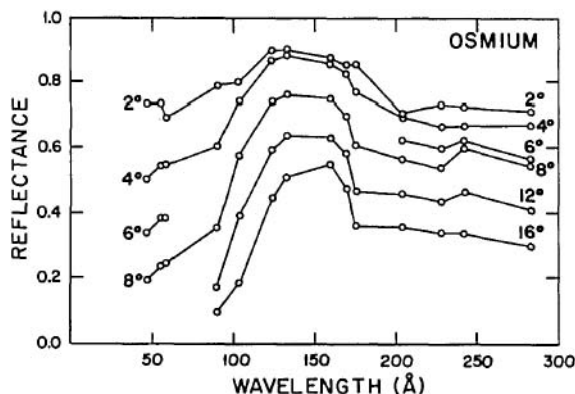


Fig. 2 Measured reflectance of osmium as a function of wavelength (46–283 Å) and graze angle (2–16°). The measurement error is estimated to be  $\pm 10\%$  relative.

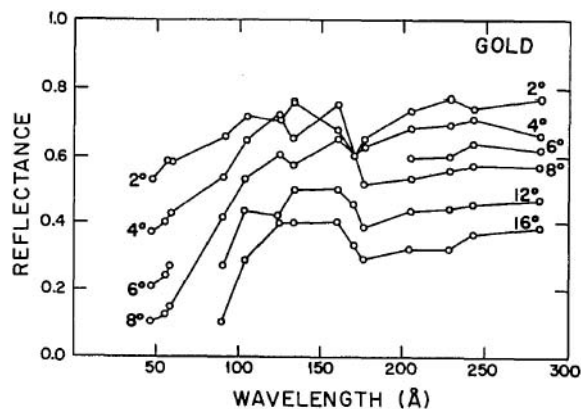


Fig. 4 Measured reflectance of gold as a function of wavelength (46–283 Å) and graze angle (2–16°). The measurement error is estimated to be  $\pm 10\%$  relative.

systematic decrease in reflectance by from 4 to 24% absolute. A typical value obtained was 8% lower than the original data plotted in Fig. 1. Measurements repeated after another 6 months, however, showed little further change in reflectances. After 4 months osmium was remeasured at 2° and for wavelengths between 47 and 175.6 Å. It showed a 5–16% decrease in reflectance. After another 2 months, the reflectance at 55.7 Å had continued to degrade to 18% lower than the initial results. A similar degradation (14.5%) appeared in measurements made at 47 Å. All the longer wavelength data (204–283 Å) were obtained several months after the initial measurements in the shorter wavelength region (47–175.6 Å). We are currently repeating the reflectance measurements for gold and platinum to determine possible degradation. It is not known whether the degraded reflectances measured for rhodium and osmium as a function of time were due to intrinsic properties of the coating, the preparation and storage of the samples, or systematic changes in the reflectometer between measurements. These degradations were not clearly correlated with either the wavelength or graze angle. Due to the importance of such coatings for space instrumentation and synchrotron radiation, further investigation into this issue is imperative.

We wish to acknowledge initiation of this project and its continued support at Acton Research Corp. by Bruce K. Flint and thank Robert Fancy at ARC for the design of the

system used to obtain these measurements. We also acknowledge helpful discussions with Anthony Hacker at Rutherford Laboratory. MCH was supported in part by the U.S. Department of Energy (contract DE-AC03-76SF00098) and by the National Aeronautics and Space Administration (contract NASW-3636).

## References

1. J. H. Weaver, C. Krafka, D. W. Lynch, and E. E. Koch, "Physik Daten, Physics Data, Optical Properties of Metals I: The transition,  $0.1 < h\nu < 500$  eV," and "Physik Daten, Physics Data Optical Properties of Metals II: Noble Metals, Aluminium, Scandium, Yttrium. The Lanthanides and the Actinides,  $0.1 < h\nu < 500$  eV," Fach-information-Zentrum, Karlsruhe (1981).
2. B. L. Henke, P. Lee, T. J. Tanaka, R. L. Shimabukuro, and B. K. Fujikawa, "Low-energy X-Ray Interaction Coefficients: Photoabsorption, Scattering, and Reflection," *At. Data Nucl. Data Tables* 27, 1 (1982).
3. J. T. Cox, G. Hass, and W. R. Hunter, "Optical Properties of Evaporated Rhodium Films Deposited at Various Substrate Temperatures in the Vacuum Ultraviolet from 150–2000 Å," *J. Opt. Soc. Am.* 61, 360 (1971).
4. W. R. Hunter, D. W. Angel, and G. Hass, "Optical Properties of Evaporated Platinum Films in the Vacuum Ultraviolet from 220 Å to 150 Å," *J. Opt. Soc. Am.* 69, 1695 (1979).

5. A. P. Lukirskii, E. P. Savinov, O. A. Ershov, and Yu F. Shepelev, "Reflection Coefficients of Radiation in the Wavelength Range from 23.6 to 113 Å for a Number of Elements and Substances and the Determination of the Refractive Index and Absorption Coefficient," *Opt. Spectrosc* 16, 168 (1964).
6. A. P. Lukirskii, E. P. Savinov, O. A. Ershov, I. I. Zhukova, and V. A. Fomichev, "Reflection of X-rays with Wavelengths from 23.6 to 190.3 Å. Some Remarks on the Performance of Diffraction Gratings," *Opt. Spectrosc* 19, 237 (1965).
7. R. F. Malina and W. Cash, "Extreme Ultraviolet Reflection Efficiencies of Diamond-turned Aluminum, Polished Nickel, and Evaporated Gold Surfaces," *Appl. Opt.* 17, 3309 (1978).
8. B. K. Flint and A. K. Hagenlocher, "Investigation of Soft X-ray Reflective Coatings," DOE/DP40156-1 (1983).
9. J. Roemer, diplomarbeit, Hamburg (1970).
10. E. D. Palik, Ed. *Handbook of Optical Constants of Solids* (Academic, Orlando, 1985), pp. 275-358.
11. W. R. Hunter and G. Hass, "Thickness of Absorbing Films Necessary to Measure Their Optical Constants Using the Reflectance-vs-Angle-Of-Incidence Method," *J. Opt. Soc. Am.* 64, 429 (1974).
12. D. S. Finley, S. Bowyer, F. Paresce, and R. F. Malina, "Continuous Discharge Penning Source with Emission Lines Between 50 Å and 300 Å," *Appl. Opt.* 18, 649 (1979).
13. P. Predehl, H. Braeuning, H. Kraus, and J. Truemper, "Fabrication of Transmission Gratings for Use in X-Ray Astronomy," *Proc. Soc. Photo-Opt. Instrum. Eng.* 316, 128 (1981).
14. M. C. Hettrick, S. Bowyer, R. F. Malina, C. Martin, and S. Mrowka, "The Extreme Ultraviolet Explorer Spectrometer," *Apl. Opt.* 24, 1737 (1985).

## Laser-induced buckling of a thin free-standing crystal film

Noel A. Clark, Phillip W. Young, and James F. Scott

University of Colorado, Physics Department, Condensed Matter Laboratory, Boulder, Colorado 80309.

Received 6 October 1984.

0003-6935/85/223685-02\$02.00/0.

© 1985 Optical Society of America

In this letter we describe a novel laser-induced instability—the thermomechanical buckling of a thin free-standing elastic plate—and the associated optical effects which allow for its ready detection and potential use.

The geometry of the experiment is illustrated in Fig. 1. A cw argon laser beam ( $\lambda = 514$  nm), focused to a 40- $\mu$ m diam beam waist, was directed at near normal incidence onto a very thin crystalline mica film. The mica films, having thickness  $t$  in the range  $0.1 \mu\text{m} < t < 0.3 \mu\text{m}$ , were prepared by cleaving high quality mica. Films of uniform thickness in this range were obtained over areas of  $5 \times 5$  mm, as evidenced by uniform white light reflection and birefringence interference colors. The films were self-supporting and generally attached to a thicker mica piece which could be conveniently mounted. The films were not held globally flat but locally were sufficiently flat that for low laser power the beam reflected from the film was nearly that expected from the diffraction limit of the incident convergent light reflected from a planar surface at the beam waist.

For a given film an abrupt change in the divergence of light reflected from the film occurred as the laser power was increased beyond a threshold power  $P_c$ . Above this threshold the reflected light became markedly divergent, indicating the onset of curvature of the reflecting surface. Two

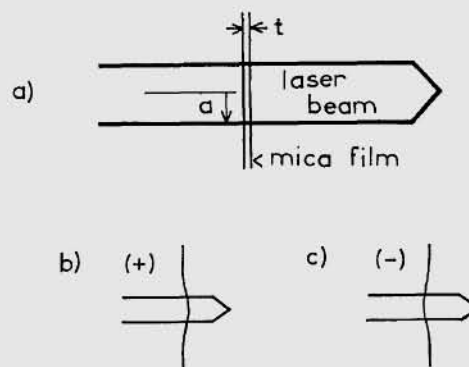


Fig. 1. (a) Experimental geometry. A thin ( $t \sim 0.2$ - $\mu\text{m}$ ) mica film is illuminated by a focused argon laser beam ( $a \sim 20 \mu\text{m}$ ). (b), (c) Above a threshold incident laser power, the film buckles into either the + or - states, which are degenerate in an initially planar film. The buckling is detected by the defocusing of the reflected light.

distinct surface curvature states were found, one positive (concave toward the incident light direction) and one negative (convex toward the incident light direction).  $P_c$  increased with increasing film thickness.

If we consider the idealized geometry of Fig. 1, with a laser beam of intensity profile  $I(x,y)$  incident along  $z$ , these observations may be interpreted as follows. Mica is optically absorbing (absorption length  $l$ ) so that passage of the laser beam is accompanied by local heating and consequent thermal expansion. For a thin plate, thin meaning that  $t \ll l$  and further that  $t \ll a$ , where  $a$  is the radius of the illuminated area, the power per unit volume deposited in the film will be  $I(x,y)/l$ , independent of  $z$ , and once thermal equilibrium is established the temperature rise distribution  $T(x,y)$  will also depend significantly only on  $x$  and  $y$ . This temperature rise will produce in-plane stresses and consequent strains in the  $x$ - $y$  plane, which, if sufficiently large, will induce buckling of the plate (displacement of the plate along  $z$ ) as indicated in Fig. 1(b) and (c). This instability is well known in the elastic theory of thin stressed plates.<sup>1</sup>

For an initially perfectly planar plate this buckling instability is doubly degenerate, as there are two (+, -) degenerate deformations that can break the initial mirror symmetry about the sample midplane. In the +(-) state the film will behave as a concave (convex) reflector. If the film is initially nonplanar and has a net Gaussian curvature in the absence of laser heating, this degeneracy will be lifted, and the laser-induced deformation will in general act to reduce the radius of the equilibrium curvature. Hence films having opposite directions of initial curvature will buckle in opposite directions. This degeneracy lifting leads to an interesting hysteresis effect in films of spatially nonuniform curvature. Consider the film in Fig. 2(a) having both positive and negative curvature regions in the absence of heating. Illuminating the concave part of the film with sufficient intensity will form a concave dimple [Fig. 2(a)]. Once established this positive dimple can be moved to and maintained on the negative region of the film by displacing the laser beam [Fig. 2(b)]. However, reducing or interrupting the laser beam or moving the dimple to a region of excessively negative curvature will produce a rapid transition to the negative state. Equivalent remarks apply for the creation and motion of a negative dimple [Figs. 2(c) and (d)]. This hysteresis effect was readily observed for laser displacements of several hundred micrometers.